

A Practical Example of the Correction of Fourier Transform Spectra for Detector Nonlinearity

M. C. Abrams and G. C. Toon and R. A. Schindler
Jet Propulsion Laboratory, California Institute of Technology
Pasadena, Ca., 91109, U.S.A.

Proposed Journal: *Applied Optics*

10 August 1993

Abstract

HgCdTe photoconductive detectors can display a nonlinear response when illuminated. In interferometric applications, this behavior must be accounted for in the data transformation process to avoid errors in the measurement of the spectral distribution of the incident radiation. A model for the distortion of the interferogram is proposed and applied to solar and atmospheric observations made by the Atmospheric Trace Molecule Spectroscopy (ATMOS) Fourier transform spectrometer during orbital sunrise and sunset from the space shuttle. Empirical estimation of the DC current level is necessary for this instrument, and satisfactory nonlinearity correction is obtained for several of the primary ATMOS optical filters. For ATMOS broadband optical filters that cover more than one-half of the alias bandwidth, the model is inadequate due to the presence of anti-aliasing electronic filters within the instrument, and it is necessary to resort to estimation and subtraction of the residual baseline offset. In either case the remaining baseline offsets are typically smaller than 1%, which is satisfactory, although it remains a significant systematic source of error in the estimation of the abundance of telluric and solar constituents from the spectra.

1. Introduction

In an ideal photometric detector, the measured signal is linearly proportional to the incident flux of radiation; in practice photoconductive infrared Mercury-Cadmium-Telluride (HgCdTe) detectors can display a nonlinear response when illuminated. Bartoli *et. al* (1974) has demonstrated that for photon fluxes in excess of 10^{19} photons-cm⁻²·sec⁻¹ the minority lifetime in photoconductive HgCdTe is not linearly proportional to the photon flux Φ , but rather to $\Phi^{-2/3}$, producing an electrical conductivity proportional to the cube root of the photon flux. Kinch and Borrello (1975) and Borrello (1977) have demonstrated that this behavior is consistent with Auger recombination of carriers within the detector. Schindler (1986) has further demonstrated that series resistance can cause the measurement to be nonlinear regardless of the illumination of the detector. For a voltage-biased photoconductive detector, the voltage output in response to a photon flux Φ is

$$\Delta V = \frac{K_1 \Phi}{(1 + K_2 \Phi)} \quad (1)$$

where K_1 and K_2 are constants that depend on the optical throughput and the circuit parameters. While it is generally the case that $K_1 \gg K_2$, at the high fluxes typical of an interferometer, the response can rarely be assumed to be linear. In either case, the measured signal is not a linear representation of the incident photon flux, and must be corrected in some fashion to properly represent the distribution of radiation.

In interferometric systems linearity is important because the measured signal is an interference pattern in which constructive and destructive superposition of the radiation near zero optical path difference produces a widely varying signal in which the modulation about the DC level contains the information about the spectral lines in the spectrum, and the central fringe contains the information about the shape of the continuum and the filter response. If the central fringe amplitude is distorted by nonlinearity in the detection and sampling process, then the quality of the resulting transform will be greatly reduced; the zero-level may be offset within the spectral bandpass, and out-of-band spectral artifacts may be introduced into the spectrum. The typical solution is to restrict the photon flux, by attenuating the incident radiation, or restricting the spectral range, or both, which may provide an unsatisfactory degradation in the signal to noise ratio and the measurement capability. An alternate solution is to develop a model of the instrumental transfer function, which can be used to correct the measured interferogram before transformation.

We propose a model based on the expected behavior of the detector and have expanded this concept in a power series expansion in the form of multiple correlations of the interferogram. In practice, interferograms can be substantially corrected to remove the detector and electronic nonlinearity; however, the aliasing of nonlinear harmonics places a restriction on the limits of the spectral bandpass that can be adequately corrected. We examine these problems in the light of the practical requirements provided by the ATMOS, which is space qualified and flies aboard a space shuttle on a near annual basis to study the Earth's atmosphere. Flight requirements and schedules prevent the redesign of the

detector and signal processing electronics to take advantage of developments made in the last decade since its design and fabrication.

The implications of nonlinear detector response in absorption spectroscopy have been examined in several previous works. Chase (1984) demonstrated a convenient method of detecting and removing the nonlinearity based on an autocorrelation of the observed spectrum. The interaction between phase correction and nonlinearity correction was illustrated with synthetic data. Practical application of the method with experimental data was not included and in particular the issue of aliasing was unaddressed. Guelachvili (1986) developed a new method for removing nonlinearity from two-output Fourier transform spectrometers by combining the modulated outputs, which have the same amplitudes and opposite phases, in a manner in which the nonlinear signal cancels itself out. This would be a highly desirable solution but is not applicable to an existing single detector instrument. Schindler (1986) proposed a nonlinearity correction circuit for photoconductive detectors which compensated for series resistance with the result being a linear measurement of the conductivity. Carter, Lindsay and Beduhn (1990) illustrated a reduced nonlinear response from HgCdTe detectors by changing the detector biasing from constant current to constant voltage, which significantly alters the detector response, but does not further address the fundamental problem for constant current biased detectors.

2. The ATMOS Fourier transform spectrometer

The Atmospheric Trace Molecule Spectroscopy (ATMOS) instrument is a high resolution Fourier transform spectrometer which measures solar spectra from the space shuttle during orbital sunset and sunrise. From the atmospheric absorptions in these spectra the structure and composition of the middle and upper atmosphere are derived (Farmer *et. al* (1987)). Within the ATMOS instrument, interferometrically modulated solar radiation is focussed onto a HgCdTe photoconductor (2 - 16 μm), with mean flux levels between 2×10^{20} and 10×10^{20} photons $\cdot cm^{-2} \cdot sec^{-1}$, depending on the field of view and the optical bandpass filter selected. These spectra display spectral artifacts that are indicative of nonlinear distortion of the interferogram in the detection and sampling process. Nearly all spectra have large spectral features between the low frequency detector cutoff at $450 cm^{-1}$ and zero frequency which Chase (1986) has demonstrated are typical of spectra obtained with poor detector linearity and may be described in terms of the autocorrelation of the intended spectrum. Spectral artifacts at frequencies larger than the high frequency cutoff of the optical filter and in-band zero offsets beneath saturated spectral features are indicative of higher order nonlinear response in the detector and sampling process.

In-band spectral offsets introduce systematic errors in the measured equivalent width of absorption lines. For ground-based or high airmass spectra with saturated absorption features it is possible to empirically correct for the offset of the zero baseline, but for upper atmospheric and solar spectra such methods are ineffective because all of the absorption features are weak and there is no way to estimate zero offsets within the spectral bandpass of the filter. Out of band spectral artifacts are observed in all spectra and may affect the assay of atmospheric or solar constituents by altering the absolute

photometric distribution. If the optical bandpass includes the upper half of the spectral alias, the non-linear response of the detector will be aliased, or folded back, into the optical bandpass and introduce additional intensity offsets.

Figure 1 illustrates high sun spectra obtained with several of the ATMOS optical filters covering portions of the 0 - 3950 cm^{-1} first-order alias bandwidth. The filters were selected to cover the bandpass between the 450 cm^{-1} cutoff of the HgCdTe detector and the alias cutoff at 4000 cm^{-1} with the purpose of preventing the short wavelength photon noise from degrading the weaker long wavelength signals. Filter 1 covers the spectral region between 450 cm^{-1} and 1150 cm^{-1} , filter 2 covers the region between 950 and 2050 cm^{-1} and filter 3 covers the region between 1550 and 3450 cm^{-1} . In terms of the alias bandwidth, the filters cover approximately one-eighth, one-quarter, and one-half of the alias width respectively, with filter 3 lying mostly in the upper half of the alias. Several features are significant and noteworthy: (a) each of the spectra contain a large low frequency feature that resembles a triangle, (b) the filter 1 and 2 spectra contain spectral artifacts at twice the respective central frequencies which are a significant component of the total spectral flux (area beneath the curve), (c) the filter 1 spectrum contains a spectral artifact at three-times the central frequency of that filter, (d) filter 3 appears relatively clean in comparison with filters 1 and 2 until it is realized that the artifacts at twice and thrice the central frequency of 2600 cm^{-1} must be folded back into the spectrum and lie at apparent frequencies of 2800 and 200 cm^{-1} respectively. Additionally, as the filter width is increased the width of the artifacts increases as well.

3. Methods

We propose a correction strategy based on a model of nonlinearity resulting from a reduction in the photoresponsivity of the detector due to Auger recombination which defines a particular shape for the nonlinear response curve of the detector. Practically, the model only provides a plausibility argument for a curve with which the actual measured interferograms can be manipulated. Additional considerations such as saturation effects would also produce nonlinear response curves, and in practice we cannot rule out the possibility that the correction strategy proposed does not also include empirical corrections for non-detector signal distortions. Unfortunately, we are constrained to working with a filtered and sampled measurement of the true detector photoconductivity and not the actual conductance produced in the detector.

A hypothetical detector response curve exhibiting detector nonlinearity is illustrated in Figure 2. The abscissa represents the absolute magnitude of the photon flux and the ordinate represents the DC detector current. Beneath the x-axis is a representation of an interferogram; under ideal conditions, the flux would range from 0 to twice the DC flux level Φ_0 , but in practice the modulation efficiency is less than unity as suggested by the curve. To the left of the y-axis is a representation of the measured interferogram after distortion by the nonlinear detector.

Let us assume that the interferogram is proportional to the cube root of the flux:

$$I(x) = a\Phi(x)^{\frac{1}{3}} \quad (2)$$

and consequently, the DC term is $I_0 = a\Phi_0^{\frac{1}{3}}$ where a is an unknown constant of proportionality. In an AC coupled single detector interferometer, the measured quantity is $I_{AC} = I - I_0$, from which we desire to recover the true representation of the interferogram on the incident flux scale which we may estimate as

$$[I(x) - I_0]_{TRUE} = [\Phi(x) - \Phi_0(x)] / \left[\frac{\partial \Phi(x)}{\partial I(x)} \right]_{I_0}. \quad (3)$$

Since $\Phi - \Phi_0 = (I/a)^3 - (I_0/a)^3$ and $(\partial \Phi / \partial I)_{I_0} = 3I_0^2/a^3$, the renormalized interferogram is

$$[I(x) - I_0]_{TRUE} = I_{AC}(x) \left[1 + \frac{I_{AC}(x)}{I_0} + \frac{1}{3} \left[\frac{I_{AC}(x)}{I_0} \right]^2 \right]. \quad (4)$$

Immediately, one observes that away from the central fringe $I_{AC} \ll I_0$ and the expression reduces to I_{AC} which simply reflects that fact that the flux variation about the DC level is small far from the central fringe and consequently the nonlinear distortion is minimal. The only unknown in the expression for the corrected interferogram is the DC detector current I_0 , since the constant of proportionality a cancels out.

Such a model will be recognized as being closely related to a generalized power series expansion of the interferogram of the form

$$I_{OBS}(x) = I(x) + \alpha I^2(x) + \beta I^3(x) \dots \quad (5)$$

where x is the path difference with respect to the location of the central fringe. A Fourier transform of such an interferogram will yield a spectrum

$$\begin{aligned} S_{OBS}(\sigma) &= \int_{-\infty}^{+\infty} I_{OBS}(x) e^{-i2\pi\sigma x} dx \\ &= \int_{-\infty}^{+\infty} I(x) e^{-i2\pi\sigma x} dx + \alpha \int_{-\infty}^{+\infty} I^2(x) e^{-i2\pi\sigma x} dx + \beta \int_{-\infty}^{+\infty} I^3(x) e^{-i2\pi\sigma x} dx + \dots \end{aligned} \quad (6)$$

in which the desired spectrum, as a function of frequency σ , is the transform of the first term, and the higher order terms are correlation harmonics, beginning with the autocorrelation

$$S(\sigma) * S(\sigma) = \int_{-\infty}^{+\infty} I^2(x) e^{-i2\pi\sigma x} dx. \quad (7)$$

When such a model is applied within the context of a discrete Fourier transform an additional complication arises: the autocorrelation of a bandpass filter will produce two spectral features corresponding to sum and difference frequencies, as illustrated in Figure 3. In the case of a relatively narrowband filter covering perhaps one-eighth of the alias width, the autocorrelation will consist of a feature near zero frequency and one at twice the central frequency of the bandpass filter. Comparison with Figure 1 indicates that there is an additional feature at three times the central frequency which is indicative of a third-order term. Broader band filters are illustrated in Figures 4 and 5, covering one-quarter and one-half of the alias width respectively. As the filter bandpass is increased the high frequency harmonic features cross the alias frequency and are folded back into the spectrum.

4. Implementation and Application

A nonlinearity correction must be applied to the raw interferogram before the initiation of the phase correction and Fourier transformation because the correction will alter the form of the interferogram immediately around the central fringe. The magnitude and location of the absolute maximum value may change and consequently alter the phase operator and hence the symmetry of the interferogram. Therefore, the nonlinearity correction must be implemented before the phase evaluation and interferogram symmetrization to avoid biasing the phase spectrum with phase features resulting from the nonlinear harmonics of the actual spectrum.

In practice the estimation of the DC current level is an empirical process, in which a series of values are chosen and utilized in the Fourier transformation process. Spectra with values of I_0 between 0 and $-2. \times 10^6$ at increments of $1. \times 10^5$ are generated. A typical occultation event will include spectra throughout orbital sunset or sunrise with widely varying atmospheric airmasses, ranging from 1.0×10^{-7} to 20 (tangent heights of 150 km to 10 km, respectively), and consequently, widely varying total flux levels and detector nonlinearity. Low sun spectra with a significant number of saturated atmospheric absorption features may have in-band offsets assessed in a straightforward manner, but high sun spectra can only be assessed in terms of the out-of-band artifacts. The resultant spectra are compared against the uncorrected spectra to evaluate the effectiveness of the parameter in changing the out-of-band artifacts and any in-band baseline offsets. A tradeoff between minimization of the out-of-band artifacts and in-band offsets is always necessary, and a compromise will have to be made. For the ATMOS instrument it is desired to determine a set of nonlinearity correction coefficients that produce an adequate correction for all flux levels. Figure 6 compares the out-of-band artifacts for ATMOS filters 1 and 2 with the lower traces illustrate the optimal correction coefficients. Figures 7 and 8 compare low sun spectra before and after correction in filters 1 and 2.

The case of ATMOS filter 3 is a special case, in that the spectral bandpass of is almost one-half of the alias width of 3950 cm^{-1} . In such a case the nonlinear harmonic information at twice and three-times the central frequency of the filter are rejected by the anti-aliasing filter in the signal processing electronics before the interferogram is sampled and recorded. The proposed model has the problem that it will introduce the harmonics and fold them back into the alias during the Fourier transform process. With an adequate measurement of the anti-aliasing filter response it should be possible to iteratively refine the nonlinearity correction. Measurements of the filter response have proved insufficient because of the sample rate which places the cutoff frequency at nearly 391.2 KHz, and circuit models of the filter, while plausible, did not provide enough information to permit successful iterative refinement of the nonlinearity correction parameter.

In the absence of a better model, we have resorted to determining the residual baseline offset and subtracting it from the spectrum after phase correction and Fourier transformation. To remove both the slope remaining from the low frequency artifact and the constant baseline offset remaining at high frequencies, two straight lines are fitted to the data in the out-of-band regions, and provided they intersect within the bandpass of the filter this provides an adequate method for removing the baseline

offsets within the filter bandpass. If the lines fail to intersect then a constant baseline offset based on the high frequency offset is all that can be applied. Typically, this approach will bring the baseline offsets to within 1% of the zero level, although some care needs to be used to avoid negative baseline offsets under saturated spectral features.

5. Conclusions

A model of a nonlinear transfer function is proposed and evaluated for removing spectral artifacts and offsets from Fourier transform spectra obtained with single HgCdTe detector interferometers. The method proves fully adequate for spectra that lie within the lower half of the spectral alias with band-passes less than or equal to one-half of the alias bandwidth. When either or both of these conditions are violated, as occurs with certain optical filters, the correction method is insufficient to remove all of the out-of-band spectral artifacts and a post transform baseline estimation and subtraction is used to remove the residual offsets.

In practice, theoretical approaches look promising, but the measured signal often seem to defy understanding and empirical correction schemes look quite tempting. Two aspects complicate modelling the nonlinear signal measured by a Fourier transform spectrometer: the nonlinear distortion predominantly affects only a few points around the central fringe and an accurate model of the electronic signal chain is essential for studying the effect of the detector nonlinearity alone. Application of a correction scheme to a filtered and sampled interferogram may or may not bear much relationship to the intended correction of the nonlinear distortion of the incident photon flux. Many years of spectroscopic evaluation of signal quality has gone into the suggested correction scheme, and during that process the model has been generalized into a power series approach in pursuit of specific improvements. In the end none of the variations proved significantly better than the initial model.

Acknowledgements

This research was performed at the Jet Propulsion Laboratory, California Institute of Technology, under a contract with the National Aeronautics and Space Administration. Much of this work is based in part on the work of the late R. H. Norton, who initially implemented and evaluated this method of nonlinearity correction for the ATMOS instrument. M. R. Gunson and R. Beer read preliminary versions of this manuscript and participated in many useful discussions about the method and its evaluation and their assistance is gratefully acknowledged. We also thank Eric Burgh, a summer student at J.P.L. in 1992 for testing our ideas on numerous examples. The technical support of J. C. Foster, J. S. Gieselman and L. L. Lowes at the Jet Propulsion Laboratory is acknowledged and greatly appreciated.

6. References

- Bartoli, F., Allen, R., Esterowitz, L., and Kruer, M., *J. Appl. Phys.*, **45**, 2150-2154, 1974.
- Borrello, S. R., *Infrared Physics*, **17**, 225-240, 1977.
- Carter III, R. O., Lindsay, N. E., and Beduhn, D., *Appl. Spectrosc.*, **44**, 1147-1151, 1990.
- Chase, D. B., *Applied Spectroscopy*, **38**, 491-494, 1984.
- Farmer, C. B., *Mikrochim. Acta (Wien)*, **III**, 189-214, 1987.
- Guelachvili, G., *Applied Optics*, **25**, 4644-4648, 1986.
- Kinch, M. A. and Borrello, S. R., *Infrared Physics*, **15**, 108-112, 1975.
- Schindler, R. A., *NASA Tech Brief*, **10**, No. 2, Item # 52, 1986.

Figure Captions

Figure 1. Uncorrected low resolution solar spectra obtained with ATMOS filters 1 and 2. Each frame contains two traces, one enlarged in the vertical by a factor of 10 to enhance the out-of-band spectral artifacts.

Figure 2. A hypothetical detector response curve exhibiting nonlinearity. The horizontal axis represents the absolute magnitude of the photon flux while the vertical axis represents the measured DC photo-current. The stylized representations of the interferograms illustrate the relative distortion of the central fringe compared to the rest of the interferogram under the assumption of 70 % modulation efficiency.

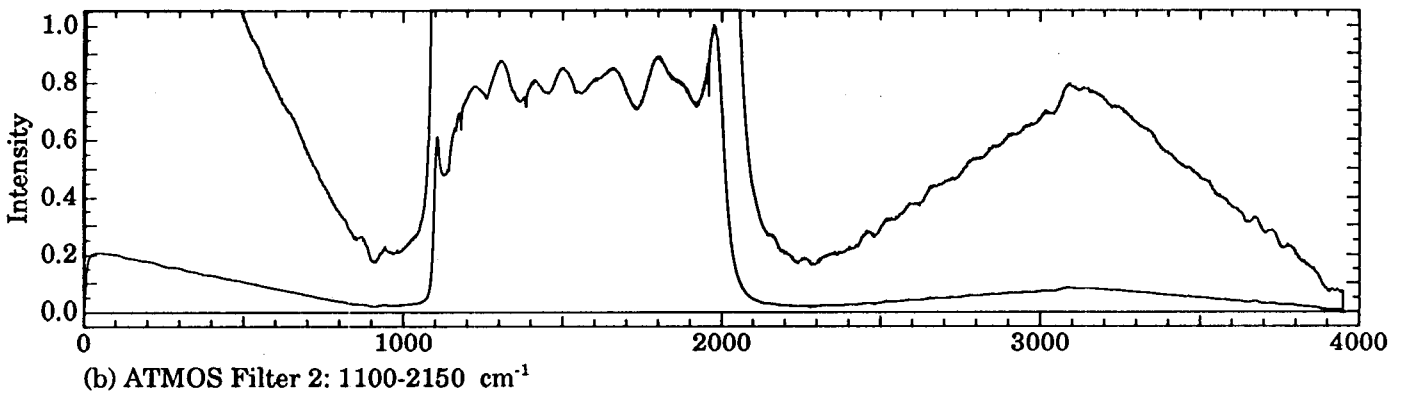
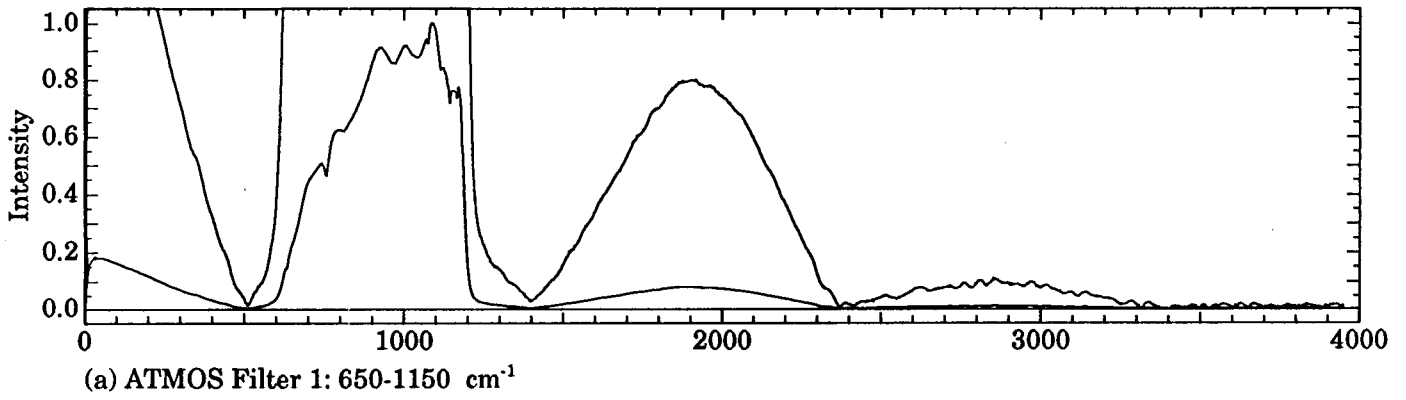
Figure 3. (a) One-eighth alias width model of ATMOS filter 1, (b) the autocorrelation of (a), (c) the cubic correlation of (a). Notice the spectral artifacts near zero frequency and twice the central frequency in the autocorrelation cases, and the feature at three times the central frequency of the filter in the cubic case. Additionally, the dominant cubic-correlation term lies within the bandpass of the filter.

Figure 4. (a) One-quarter alias width model of ATMOS filter 2, (b) the autocorrelation of (a), (c) the cubic correlation of (a). Notice the spectral artifacts near zero frequency and twice the central frequency in the autocorrelation cases, and the feature at three times the central frequency of the filter in the cubic case. Aliasing is apparent in the cubic correlation.

Figure 5. (a) One-half alias width model of ATMOS filter 3, (b) the autocorrelation of (a), (c) the cubic correlation of (a). Notice the spectral artifacts near zero frequency and twice the central frequency in the autocorrelation cases, and the feature at three times the central frequency of the filter in the cubic case. Aliasing is evident in the autocorrelation function.

Figure 6. ATMOS filters 1 and 2 high sun spectra, (a) before and (b) after nonlinearity correction.

Figure 7. ATMOS filter 1 low sun spectra - in-band comparison, (a) before and (b) after nonlinearity correction.



Abrams et al: Figure 1

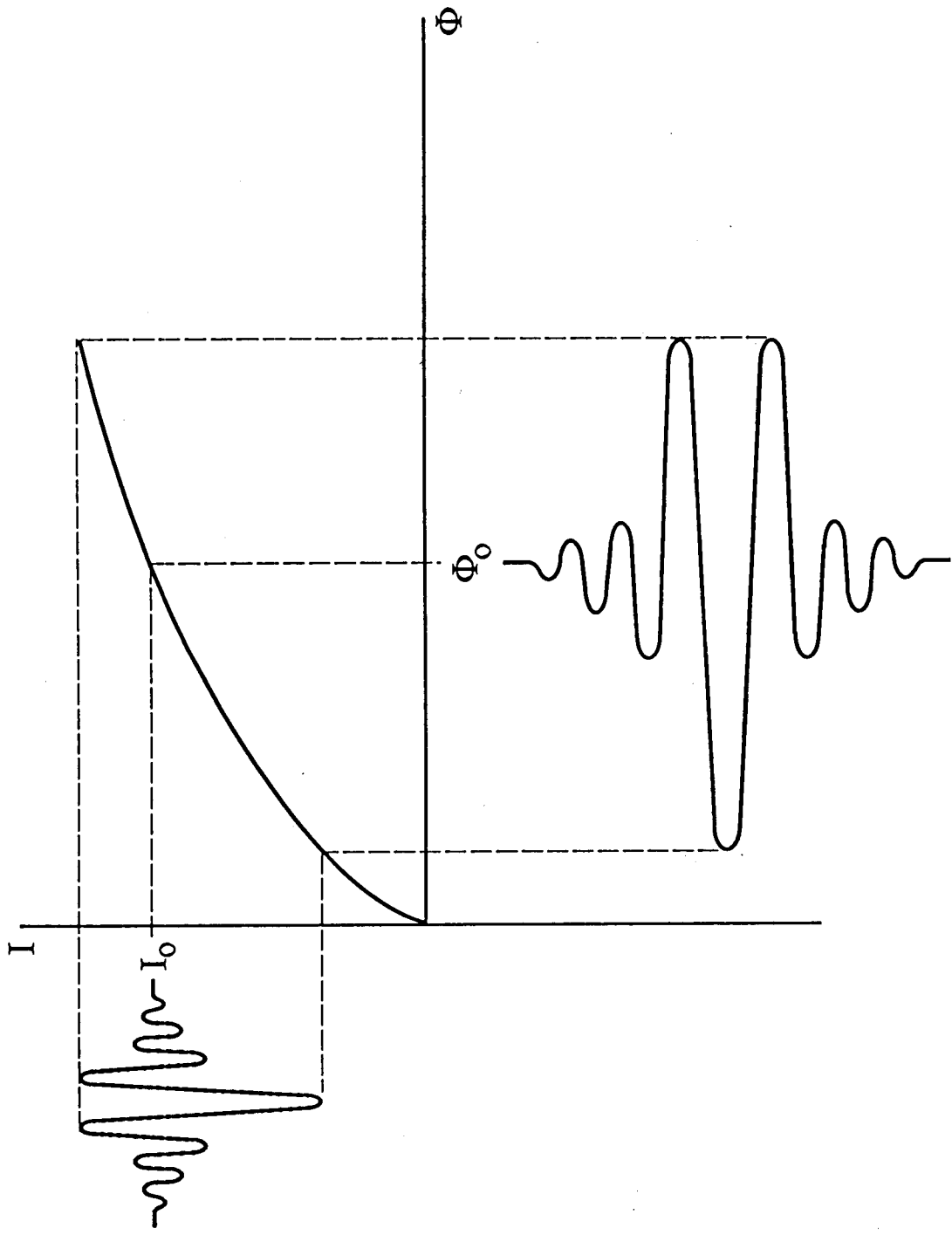
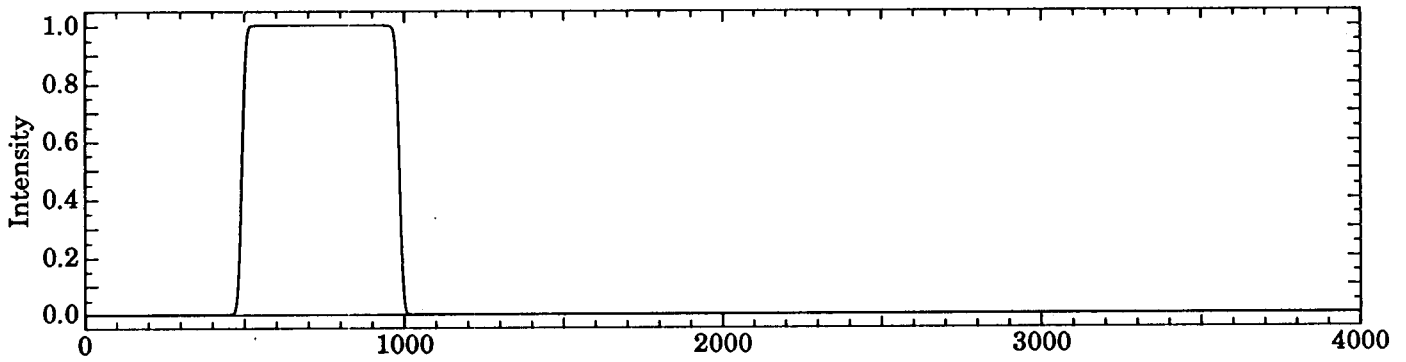
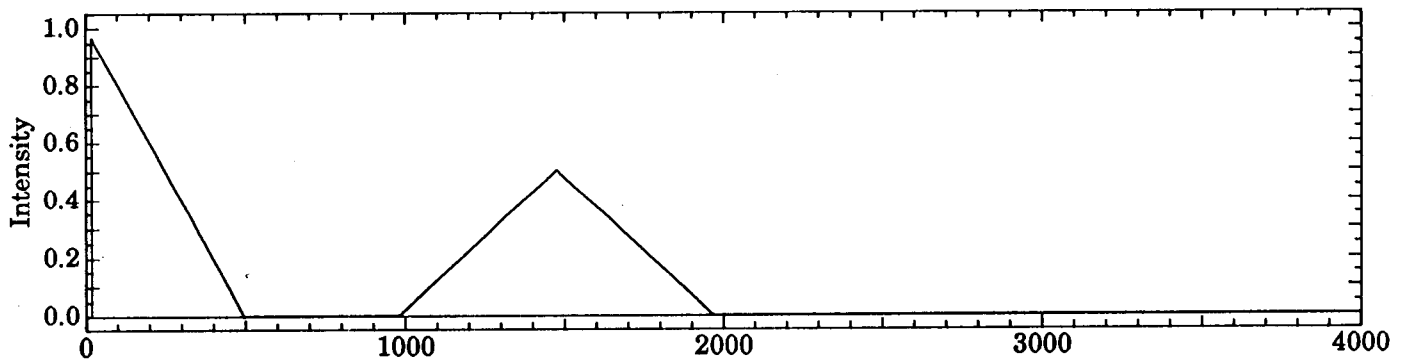


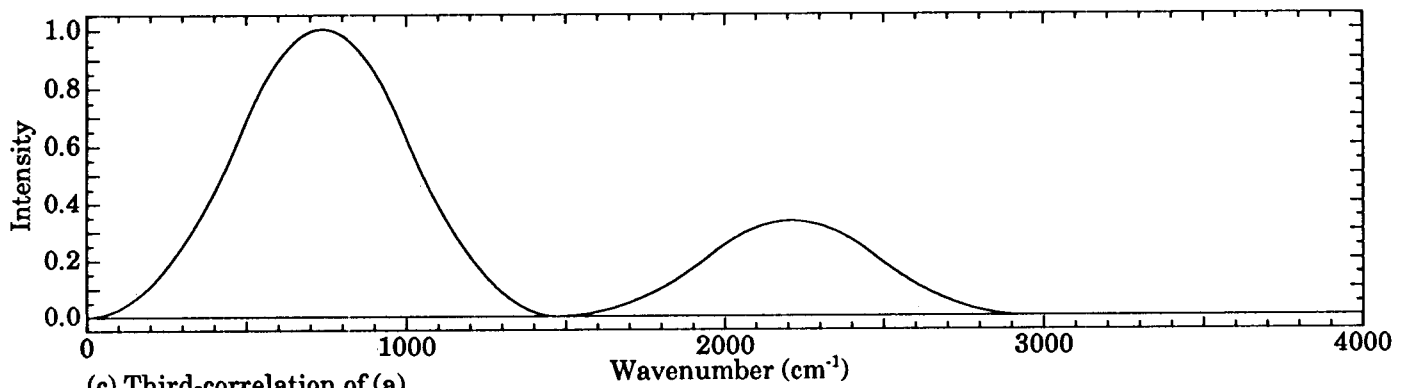
FIGURE 2



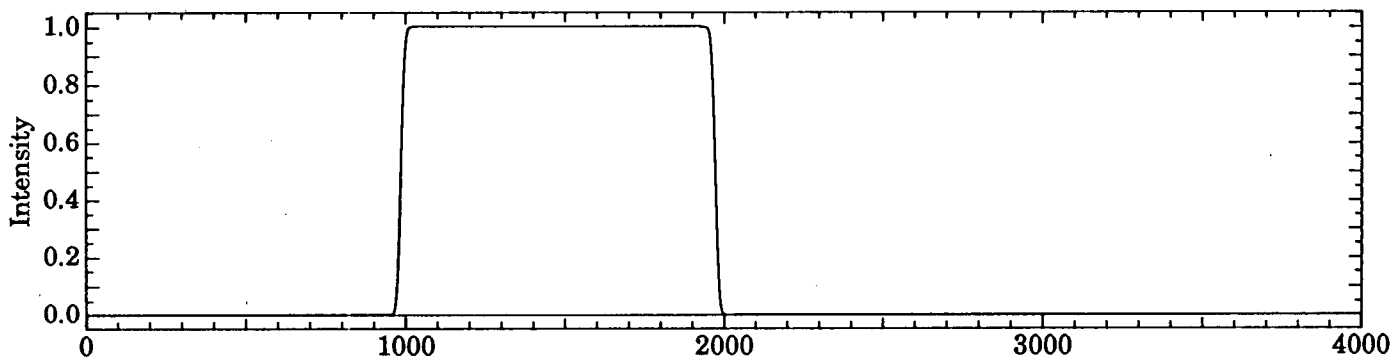
(a) One-eighth alias width filter



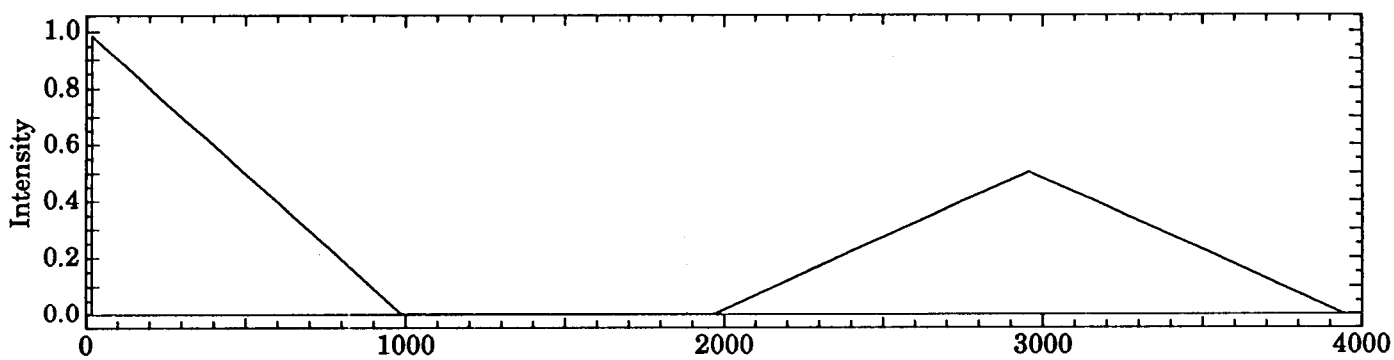
(b) Autocorrelation of (a)



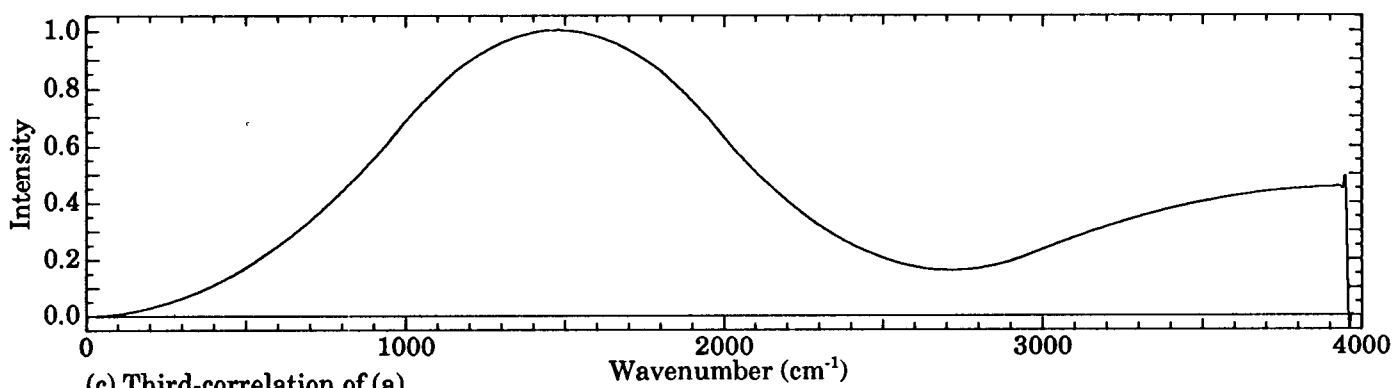
(c) Third-correlation of (a)



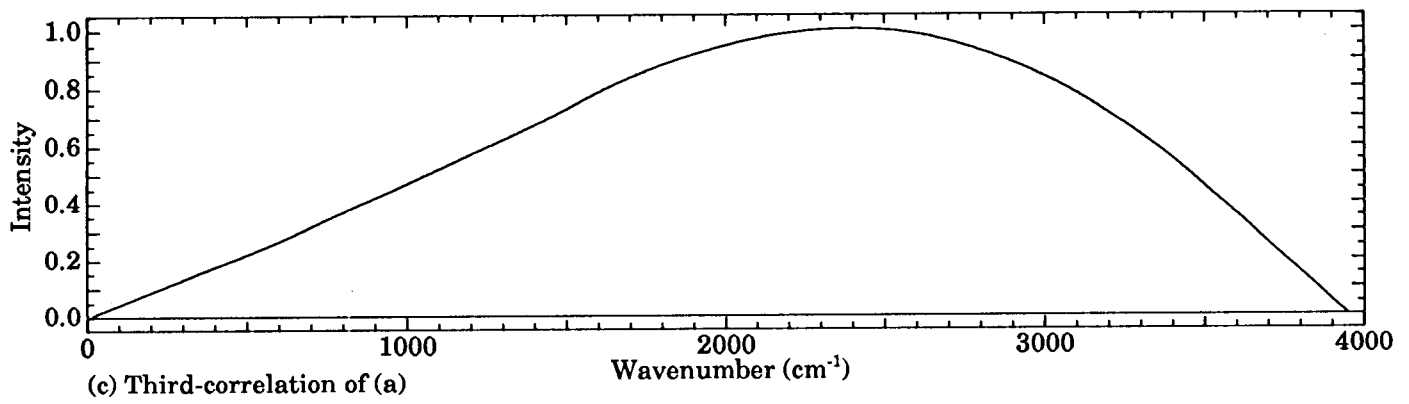
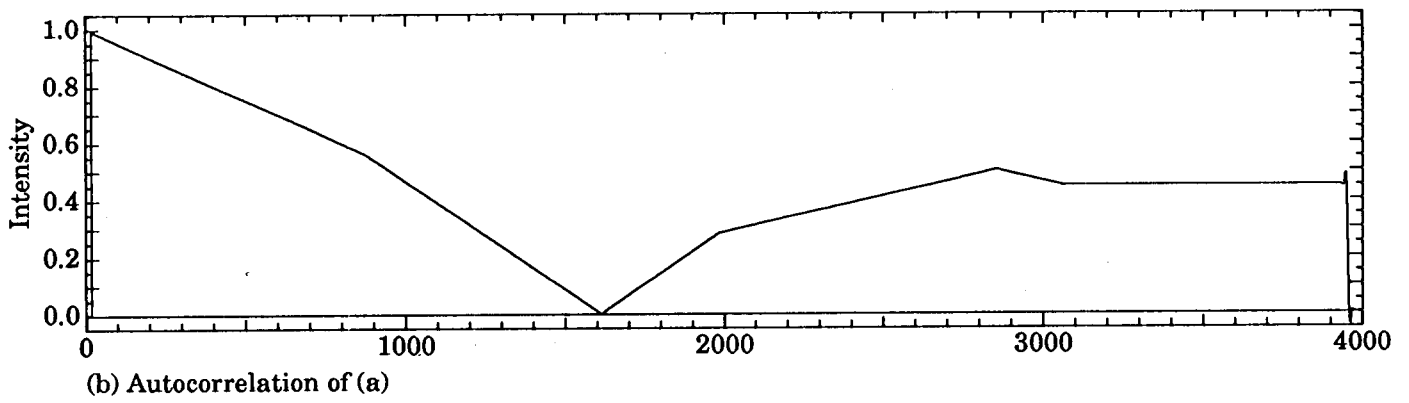
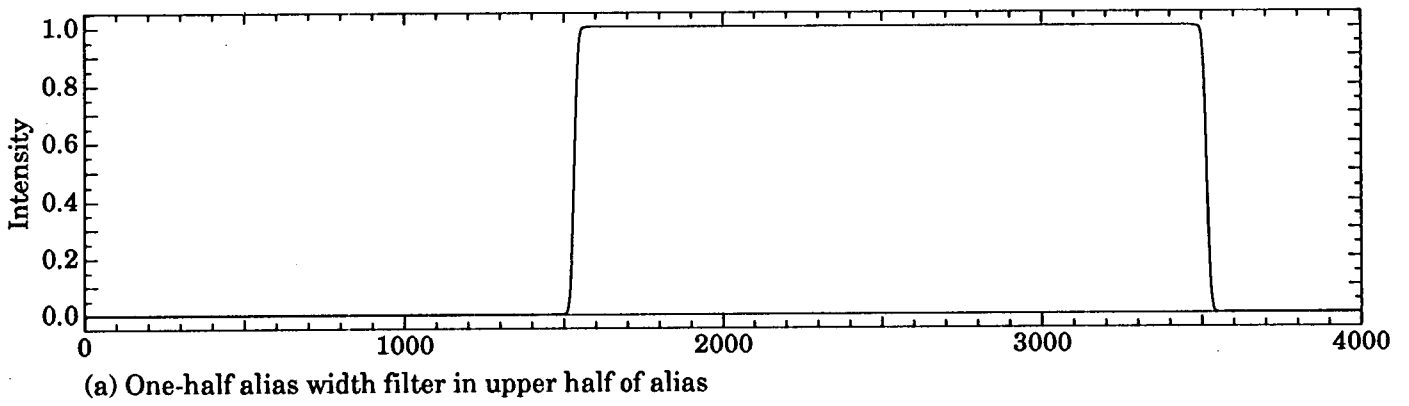
(a) One-quarter alias width filter

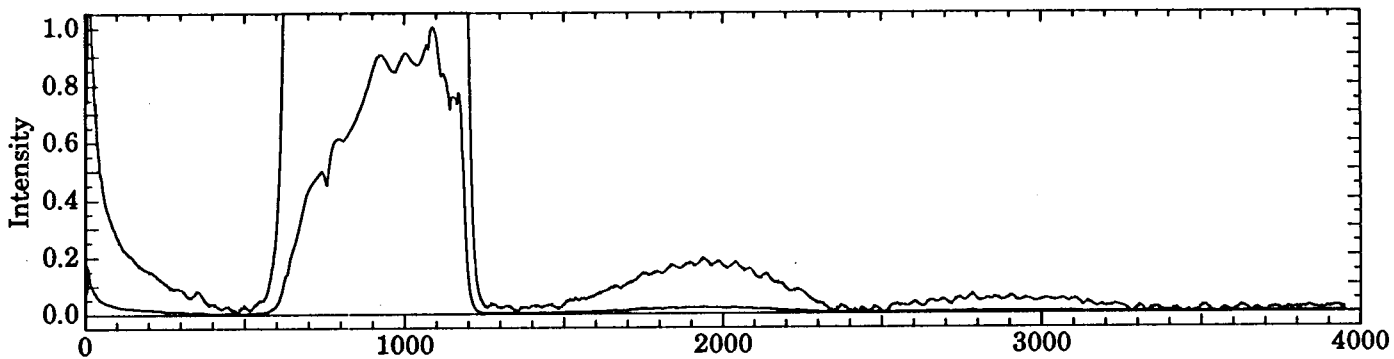


(b) Autocorrelation of (a)

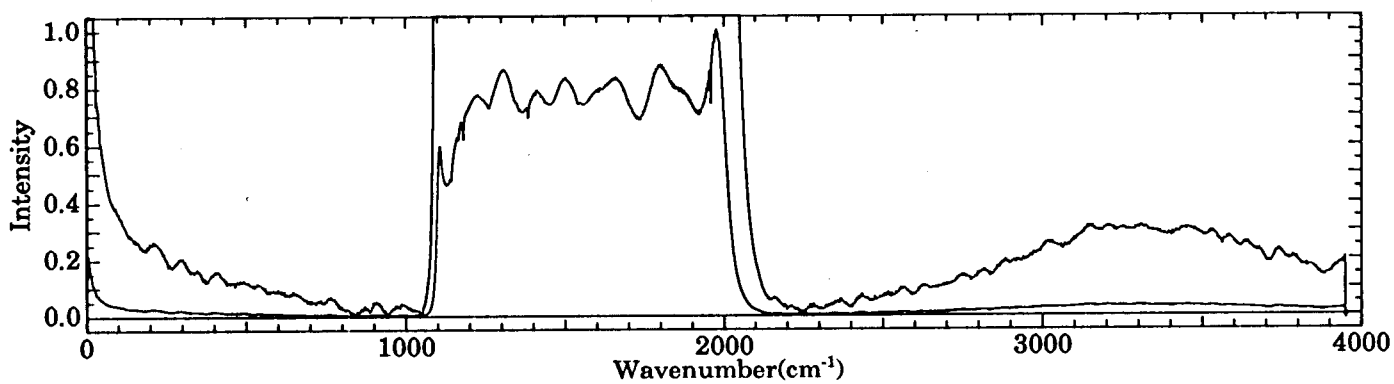


(c) Third-correlation of (a)





(a) ATMOS Filter 1: with $-1.e-6$ nonlinearity correction



(b) ATMOS Filter 2: with $-1.1e-6$ nonlinearity correction

